



Universiteit  
Leiden  
The Netherlands

## **The optimal imaging window for dysplastic colorectal polyp detection using c-met-targeted fluorescence molecular endoscopy**

Jongh, S.J. de; Vrouwe, J.P.M.; Voskuil, F.J.; Schmidt, I.; Westerhof, J.; Koornstra, J.J.; ... ; Nagengast, W.B.

### **Citation**

Jongh, S. J. de, Vrouwe, J. P. M., Voskuil, F. J., Schmidt, I., Westerhof, J., Koornstra, J. J., ... Nagengast, W. B. (2020). The optimal imaging window for dysplastic colorectal polyp detection using c-met-targeted fluorescence molecular endoscopy. *Journal Of Nuclear Medicine*, 61(10), 1435-1441. doi:10.2967/jnumed.119.238790

Version: Publisher's Version

License: [Licensed under Article 25fa Copyright Act/Law \(Amendment Taverne\)](#)

Downloaded from: <https://hdl.handle.net/1887/3270996>

**Note:** To cite this publication please use the final published version (if applicable).



# The Optimal Imaging Window for Dysplastic Colorectal Polyp Detection Using c-Met–Targeted Fluorescence Molecular Endoscopy

Steven J. de Jongh<sup>\*1</sup>, Josephina P.M. Vrouwe<sup>\*2</sup>, Floris J. Voskuil<sup>3</sup>, Iris Schmidt<sup>1</sup>, Jessie Westerhof<sup>1</sup>, Jan J. Koornstra<sup>1</sup>, Marieke L. de Kam<sup>2</sup>, Arend Karrenbeld<sup>4</sup>, James C.H. Hardwick<sup>5</sup>, Dominic J. Robinson<sup>6</sup>, Jacobus Burggraaf<sup>2</sup>, Ingrid M.C. Kamerling<sup>†2</sup>, and Wouter B. Nagengast<sup>†1</sup>

<sup>1</sup>Department of Gastroenterology and Hepatology, University Medical Center Groningen, Groningen, The Netherlands; <sup>2</sup>Centre for Human Drug Research, Leiden, The Netherlands; <sup>3</sup>Department of Oral and Maxillofacial Surgery, University Medical Center Groningen, Groningen, The Netherlands; <sup>4</sup>Department of Pathology, University Medical Center Groningen, Groningen, The Netherlands; <sup>5</sup>Department of Gastroenterology and Hepatology, Leiden University Medical Center, Leiden, The Netherlands; and <sup>6</sup>Center for Optical Diagnostics and Therapy, Department of Otorhinolaryngology and Head and Neck Surgery, Erasmus MC Cancer Institute, Rotterdam, The Netherlands

Fluorescence molecular endoscopy (FME) is an emerging technique that has the potential to improve the 22% colorectal polyp detection miss-rate. We determined the optimal dose-to-imaging interval and safety of FME using EMI-137, a c-Met–targeted fluorescent peptide, in a population at high risk for colorectal cancer. **Methods:** We performed in vivo FME and quantification of fluorescence by multidiameter single-fiber reflectance/single-fiber fluorescence spectroscopy in 15 patients with a dysplastic colorectal adenoma. EMI-137 was intravenously administered (0.13 mg/kg) at a 1-, 2- or 3-h dose-to-imaging interval ( $n = 3$  patients per cohort). Two cohorts were expanded to 6 patients on the basis of target-to-background ratios. Fluorescence was correlated to histopathology and c-Met expression. EMI-137 binding specificity was assessed by fluorescence microscopy and in vitro experiments. **Results:** FME using EMI-137 appeared to be safe and well tolerated. All dose-to-imaging intervals showed significantly higher fluorescence in the colorectal lesions than in surrounding tissue, with a target-to-background ratio of 1.53, 1.66, and 1.74 for the 1-, 2-, and 3-h cohorts, respectively, and a mean intrinsic fluorescence of 0.035 vs. 0.023 mm<sup>-1</sup> ( $P < 0.0003$ ), 0.034 vs. 0.021 mm<sup>-1</sup> ( $P < 0.0001$ ), and 0.033 vs. 0.019 mm<sup>-1</sup> ( $P < 0.0001$ ), respectively. Fluorescence correlated with histopathology on a macroscopic and microscopic level, with significant c-Met overexpression in dysplastic mucosa. In vitro, a dose-dependent specific binding was confirmed. **Conclusion:** FME using EMI-137 appeared to be safe and feasible within a 1- to 3-h dose-to-imaging interval. No clinically significant differences were observed among the cohorts, although a 1-h dose-to-imaging interval was preferred from a clinical perspective. Future studies will investigate EMI-137 for improved colorectal polyp detection during screening colonoscopies.

**Key Words:** optimal imaging window; fluorescence molecular endoscopy; colorectal polyp detection; colorectal cancer; EMI-137 targeting c-Met

**J Nucl Med 2020; 61:1435–1441**

DOI: 10.2967/jnumed.119.238790

Most colorectal cancers develop through the adenoma-to-carcinoma sequence (1). Therefore, early detection of premalignant polyps such as adenomas and sessile serrated polyps could improve patient outcome (2). To date, the gold standard for premalignant lesion detection is high-definition white-light endoscopy (HD-WLE). Although HD-WLE has significantly contributed to the success of screening for and prevention of colorectal cancer, it also has limitations (3,4). Factors such as inadequate bowel preparation and lack of skill and expertise by the endoscopist may cause reduced sensitivity, leading to an adenoma detection miss-rate of up to 22% in the general population and 55% in patients with Lynch syndrome (5,6). Certain locations (i.e., ascending colon) and morphologic characteristics of the adenoma such as small size (i.e., less than 10 mm) or flat shape are notorious for higher miss-rates (7).

These factors emphasize the need for a novel imaging technology to reduce the high detection miss-rates. Fluorescence molecular endoscopy (FME) administers targeted fluorescent tracers that enable visualization of specific markers overexpressed on the target of interest. Combining HD-WLE technique to visualize morphologic mucosal abnormalities with FME to visualize real-time biologic characteristics of cells has the potential to improve polyp detection rates (8–10).

One of the markers that becomes significantly overexpressed as the degree of dysplasia progresses in the colorectal adenoma-to-carcinoma sequence is c-Met (11). c-Met is a receptor tyrosine kinase that binds to its ligand hepatocyte growth factor and activates several downstream signaling pathways involved in proliferation, motility, migration, and invasion (11,12). The fluorescently labeled peptide EMI-137 (previously: GE-137) is a water-soluble 26-amino-acid cyclic peptide that specifically binds to human c-Met with high

Received Oct. 24, 2019; revision accepted Feb. 21, 2020.

For correspondence or reprints contact: Wouter B. Nagengast, Department of Gastroenterology and Hepatology, University Medical Center Groningen, Hanzplein 1, 9713GZ, Groningen, the Netherlands.

E-mail: w.b.nagengast@umcg.nl

<sup>\*</sup>Contributed equally to this work.

<sup>†</sup>Contributed equally to this work.

Published online Mar. 20, 2020.

COPYRIGHT © 2020 by the Society of Nuclear Medicine and Molecular Imaging.



affinity (8). It has a peak excitation and emission wavelength of 653 and 675 nm, respectively, and favorable pharmacokinetic properties that enable rapid tissue biodistribution, with a background clearance half-life of approximately 2 h 30 min.

Previously, intravenous administration of EMI-137 3 h before colonoscopy showed the potential to detect additional polyps that were initially missed by conventional fiber-based white-light colonoscopy (8). To expand the clinical applicability of EMI-137 for future phase II or III trials, we determined its optimal dose-to-imaging interval for colorectal polyp detection using FME in parallel with HD-WLE, with quantification of fluorescence using multidiameter single-fiber reflectance/single-fiber fluorescence (MDSFR/SFF) spectroscopy. In addition, the safety and tolerability of EMI-137 were investigated in a group of patients in whom colorectal cancer was strongly suspected.

## MATERIALS AND METHODS

### Study Design

This study was approved by the Foundation Beoordeling Ethiek Biomedisch Onderzoek ethics committee. All patients gave written informed consent. Patients were eligible for study participation if they were at least 18 y old and scheduled to undergo a diagnostic or therapeutic endoscopy for a colorectal adenoma containing at least low-grade dysplasia. Female patients had to be either surgically sterile, postmenopausal, or premenopausal with a negative urine pregnancy test. The study was registered in the European Clinical Trials Register (2016-002827-27) and conducted according to the Declaration of Helsinki at the University Medical Center Groningen between October 2017 and September 2018.

### In Vivo Endoscopy Procedures

EMI-137 was administered as a single intravenous bolus injection of 0.13 mg/kg in a solution of 4.8 mg/mL at either 1, 2, or 3 h before endoscopy, initially with 3 patients per cohort (Fig. 1). All endoscopic procedures were performed by a board-certified gastroenterologist using a clinical high-definition videoendoscope (CF-HQ190 L/I, Evis Exera III; Olympus Corp.) after standard bowel preparation. Therapy consisted of piecemeal polypectomy, endoscopic mucosal resection, endoscopic submucosal dissection, or endoscopic full-thickness resection, depending on lesion location, size, and characteristics. A 650-nm short-pass filter (Chroma Technology Corp.) was installed in the Olympus xenon light source (CLV-190, Evis Exera III) to prevent unintended excitation of EMI-137.

Fluorescence was visualized in vivo using the SurgVision Endoscope Explorer (SurgVision B.V.), a real-time fluorescence imaging system connected to a flexible fiberscope that can be inserted through the clinical high-definition videoendoscope. The SurgVision Endoscope Explorer consists of a white-light-emitting diode and 2 class III-b lasers optimized for EMI-137 visualization (excitation wavelength, 653 nm), which simultaneously produce a white-light, fluorescence, and overlay image.

During FME, adenoma visibility was qualitatively described as “clearly increased,” “mildly increased,” or “same as background,” compared with the surrounding normal tissue, by consensus between the gastroenterologist and the investigator. To confirm the in vivo visualized fluorescence imaging results, fluorescence intensities were subsequently quantified in vivo using MDSFR/SFF spectroscopy, an optical technique that corrects for the influence of tissue optical properties and therefore enables determination of the EMI-137 intrinsic fluorescence values (Fig. 2A). Briefly, another fiber bundle was inserted to determine the tissue absorption coefficient and reduced scattering coefficient at the excitation wavelength (650 nm) and the emission band of the fluorophore,

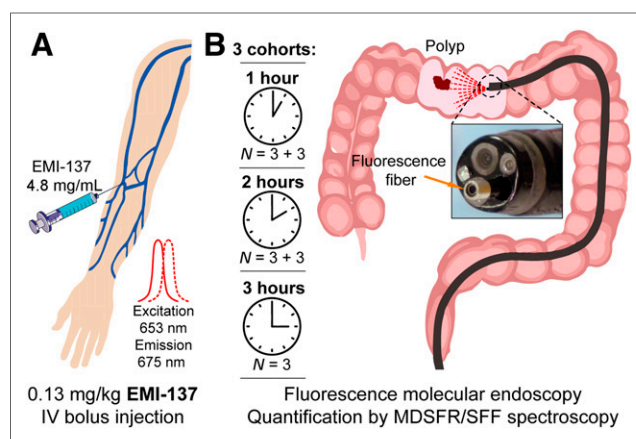


**FIGURE 1.** Study workflow. (A) EMI-137 was administered intravenously (0.13 mg/kg). (B) After 1, 2, or 3 h, real-time FME and in vivo MDSFR/SFF spectroscopy were performed. Per cohort, 3 patients were included, with expansion to 6 patients for 1- and 2-h cohorts based on interim analysis results.

cyanine-5\*\* (600–800 nm), through direct-contact MDSFR measurements. Subsequently, an SFF spectrum was acquired. After the clinical procedure, the intrinsic fluorescence values of cyanine-5\*\* in EMI-137 were calculated (10,13–15).

Depending on the endoscopy procedure length, multiple FME and MDSFR/SFF spectroscopy measurements were acquired of each lesion and the surrounding normal tissue every 30 min. If in vivo MDSFR/SFF spectroscopy measurements could not be acquired because of the lesion location (this fiber bundle cannot be inverted), measurements were obtained ex vivo directly after resection.

### Outcome Parameters

**Safety and Tolerability.** Vital signs, the injection site, and the occurrence of serious adverse events based on the Common Toxicity Criteria for Adverse Events were monitored at regular time points. Follow-up took place up to 24–48 h after EMI-137 administration.

**In Vivo Target-to-Background Ratio (TBR) Analysis.** Regions of interest for the lesion and surrounding normal colorectal tissue were delineated on 1–4 representative white-light images per patient at approximately the same distance from the fiber, depending on image availability and quality. Subsequently, mean fluorescent intensities (MFIs) were calculated as total counts per region-of-interest pixel area using Fiji/ImageJ software (version 2.0.0-rc-68/1.52h). The lesion MFI was divided by the surrounding normal-tissue MFI to determine TBRs. In addition to the FME analysis (i.e., a TBR calculation based on the MFIs of the in vivo FME images), we also evaluated the in vivo quantitative MDSFR/SFF spectroscopy data (i.e., a TBR calculation based on the quantitative intrinsic fluorescence values).

**Interim Analysis.** An interim analysis was performed after the first 9 patients to evaluate EMI-137 safety data and to determine the TBR using FME and MDSFR/SFF spectroscopy for each cohort. The 2 cohorts with the optimal TBR were expanded to 6 patients per cohort. If TBRs were comparable for all 3 cohorts, the 1- and 2-h cohorts were to be expanded to 6 patients per cohort, as a shorter dose-to-imaging interval was preferred from a clinical perspective.

### Ex Vivo Validation

After resection, histopathologic processing and examination were performed according to the standard clinical protocol of the University Medical Center Groningen by a board-certified gastrointestinal pathologist, who did not know the fluorescence imaging results.



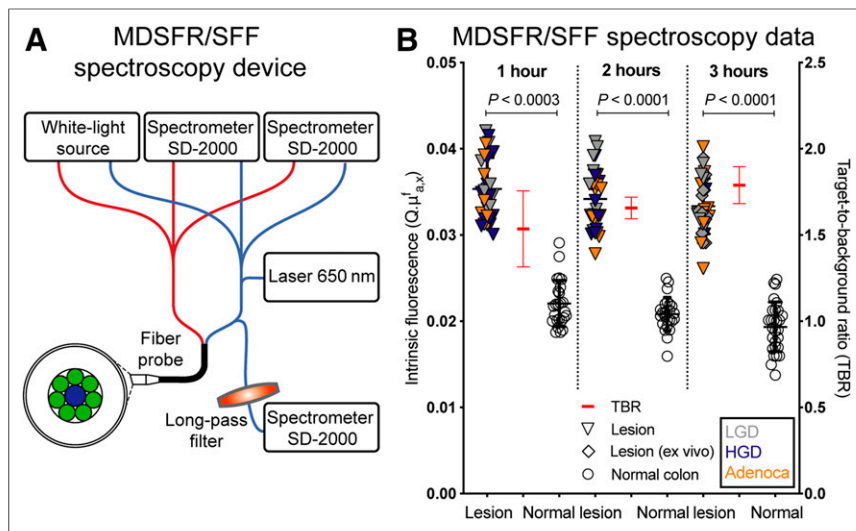


**FIGURE 2.** MDSFR/SFF spectroscopy. (A) Schematic overview of device. (B) Individual intrinsic fluorescence values of adenomas and surrounding normal tissue per time cohort (left y-axis), with mean target-to-background (TBR) ratios (red; right y-axis). Histologic grade of adenoma is low-grade dysplasia (LGD; gray), high-grade dysplasia (HGD; blue), and adenocarcinoma (Adenoca; orange). Error bars indicate mean values  $\pm$  SD.

**Correlation of Fluorescence and Histopathology.** A maximum of four 4- $\mu$ m tissue sections per patient was selected for further analyses, on the basis of section quality and the simultaneous presence of dysplasia and surrounding normal crypts. After xylene deparaffinization, tissue sections were air-dried and scanned using the Odyssey CLx fluorescence scanner (LI-COR Biosciences Inc.), directly followed by hematoxylin and eosin staining, to allow a precise correlation of fluorescence with histology. MFIs were measured as total counts per region-of-interest pixel area for dysplastic mucosa and surrounding normal mucosa based on histologic delineation by the pathologist.

**Immunohistochemistry.** A SP44 rabbit monoclonal primary antibody directed against the membranous and cytoplasmic c-Met epitope was applied to perform c-Met immunohistochemistry using the BenchMark Ultra system (Ventana Medical Systems) according to the standard clinical protocol of the University Medical Center Groningen. Membrane-localized staining intensities were semiquantitatively scored as negative (0), weak (1+), moderate (2+), or strong (3+) in dysplastic and surrounding normal colorectal mucosa by the pathologist. A 2+/3+ score was considered positive for c-Met overexpression.

**Fluorescence Microscopy.** Fluorescence microscopy was performed on 1 representative 4- $\mu$ m tissue section per patient, to evaluate the accumulation of EMI-137 on a microscopic level, as described previously (15,16). A DM6000 fluorescence microscope coupled to a DFC360FX camera (Leica Biosystems GmbH) was applied using the same settings per magnification on the A (fluorescein isothiocyanate, autofluorescence), I (4',6-diamidino-2-phenylindole, nuclei), and Y5 (cyanine-5; i.e., EMI-137) filter cube.

**Validation Side Study.** Several in vitro experiments were performed on a highly c-Met-overexpressing cell line (HT-29) and on a cell line negative for c-Met expression (SW-480) to confirm the specificity of EMI-137 binding (described in the supplemental materials, available at <http://jnm.snmjournals.org>) (17).

### Statistical Analysis

Descriptive statistics were applied to the patient demographics. Normally distributed data are presented as mean value with SD, and a Student *t* test (paired data) was used to test for significance. Nonnormally distributed data are presented as median value with interquartile range

(IQR), and a Wilcoxon (paired data) or Mann-Whitney U (independent data) test was used to test for significance. *P* values of less than 0.05 were considered statistically significant. Statistical analyses and graph design were performed using GraphPad Prism (version 8.0; GraphPad Software Inc.).

## RESULTS

### Study Population

In total, 19 patients gave written informed consent and were screened for study participation, and 16 were found eligible for inclusion. The mean age was 62 y (range, 59–73 y; Table 1). All 16 patients received an intravenous-bolus 0.13 mg/kg injection of EMI-137. Fourteen patients underwent an intended therapeutic procedure (3 piece-meal polypectomies, 4 endoscopic mucosal resections, 6 endoscopic submucosal dissections, and 1 endoscopic full-thickness resection), 1 patient underwent a diagnostic procedure, and in 1 patient the colonoscopy was prematurely aborted because of the patient's discomfort. Histologic assessment of the resected lesions showed all to be tubular adenomas that contained at least low-grade dysplasia. High-grade dysplasia was present in 5 tubular adenomas (31.2%), and adenocarcinoma was present in another 3 lesions (18.8%; Table 1).

### Safety and Tolerability

No clinically significant changes in vital signs were observed after administration of EMI-137 in any of the patients, nor were there any skin abnormalities at the injection site. One possibly related grade 1 adverse event (hypotension after anesthesia) and 1 possibly related grade 2 adverse event (mild allergic reaction, multiple hours after EMI-137 administration) were observed. Two serious adverse events occurred; both were iatrogenic perforations of the large intestine, which were considered not related to EMI-137 or any study-related procedures but to the therapeutic endoscopy procedure (sigmoid perforation during endoscopic full-thickness resection and rectum perforation during repeated endoscopic submucosal dissection in the area of a previously performed endoscopic mucosal resection).

### In Vivo Endoscopy Procedures

FME was performed in 15 of 16 patients. In 1 patient, the endoscopy procedure was prematurely aborted, as the cecum polyp could not be reached because of the patient's discomfort. This patient underwent polypectomy under propofol sedation at a later stage and was replaced in the study. The planned interim analysis after enrollment of the first 9 patients showed comparable TBRs for all 3 time intervals regarding FME images and MDSFR/SFF spectroscopy measurements. The 1- and 2-h cohorts were expanded to 6 patients each, because of the clinical preference for a shorter dose-to-imaging interval.

The dose-to-imaging time intervals were 0:54–1:28 h for the 1-h cohort, 1:50–2:33 h for the 2-h cohort, and 2:41–3:20 h for the 3-h cohort. In total, 16 lesions were detected during endoscopy in 15 patients. The median adenoma size estimated during colonoscopy was 3.0 cm (range, 1.5–5.5 cm). Fluorescence was qualitatively assessed in vivo as clearly increased in 5 of 16 adenomas (31%),



**TABLE 1**  
Demographics and Clinical Characteristics

Characteristic	Data
Total patients	15 (100%)
Sex	
Male	10 (66.7%)
Female	5 (33.3%)
Age (y)	62 (59–73)
Body mass index (kg/m <sup>2</sup> )	27.7 (21.6–42.7)
Time cohort	
1 h	6 (40%)
2 h	6 (40%)
3 h	3 (20%)
Endoscopy procedure	
Diagnostic	1 (6.7%)
Piecemeal polypectomy	3 (20%)
Endoscopic mucosal resection	4 (26.6%)
Endoscopic submucosal resection	6 (40%)
Endoscopic full-thickness resection	1 (6.7%)
Adenoma size (cm)	3.0 (1.5–5.5)
Histology (highest grade)	
Low-grade dysplasia	8 (50%)
High-grade dysplasia	5 (31.2%)
Adenocarcinoma	3 (18.8%)

Qualitative data are numbers followed by percentages in parentheses; continuous data are medians followed by ranges in parentheses.

mildly increased in 8 of 16 (50%), and the same as the background in 3 of 16 (19%), on the basis of the FME images. The 3 lesions that were assessed to have the same fluorescence as the background could be identified using fluorescence because of their morphologic characteristics. Representative FME images are shown in Figure 3.

In total, 74 representative FME images acquired from the 16 lesions at different time points were analyzed to determine the TBR at each time interval. All lesions showed increased fluorescence compared with surrounding normal colorectal tissue, with a median TBR of 2.18 (IQR, 0.87), 1.62 (IQR, 0.51), and 1.43 (IQR, 0.75) for the 1-, 2-, and 3-h dose-to-imaging intervals, respectively (Fig. 4).

In addition to the FME TBRs, in vivo direct-contact MDSFR/SFF spectroscopy measurements were analyzed using a postprocessing algorithm to quantify the intrinsic fluorescence values by correcting for the optical properties in 14 of 16 lesions. MDSFR/SFF spectroscopy measurements of the remaining 2 lesions were performed ex vivo directly after adenoma resection, since in vivo measurements were not feasible for technical reasons. Quantified intrinsic fluorescence was significantly higher in the adenomas than in surrounding normal tissue for the 1-h cohort ( $0.035 \pm 0.0023$  vs.  $0.023 \pm 0.0024$  mm<sup>-1</sup>,  $P < 0.0003$ ), 2-h cohort ( $0.034 \pm 0.0020$  vs.  $0.021 \pm 0.0014$  mm<sup>-1</sup>,  $P < 0.0001$ ), and 3-h cohort ( $0.033 \pm 0.0023$  vs.  $0.019 \pm 0.0023$  mm<sup>-1</sup>,  $P < 0.0001$ ; Fig. 2B). Quantified

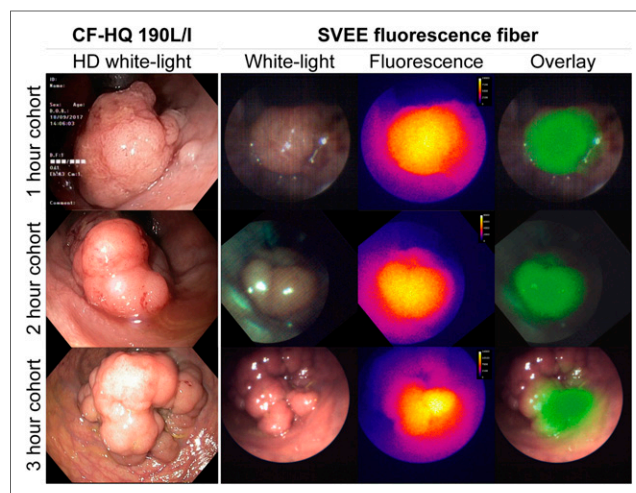


**FIGURE 3.** Representative FME images of lesion with surrounding normal tissue for each cohort. Columns from left to right are HD-WLE image (Olympus CF-HQ 190 L/I) and white-light, fluorescence, and overlay image (SurgVision Endoscope Explorer [SVEE]). Histologic grade from top to bottom is adenocarcinoma, adenocarcinoma, and low-grade dysplasia.

fluorescence values in the adenomas remained consistent from 1 h to at least 3 h. In contrast, a slight decreasing trend was observed for the quantified fluorescence values in normal colorectal tissue (Fig. 2B). As a result, the spectroscopy TBRs slightly increased over time, with a mean TBR of  $1.53 \pm 0.21$ ,  $1.66 \pm 0.07$ , and  $1.74 \pm 0.16$  for the 1-, 2-, and 3-h cohorts, respectively (Fig. 2B, right axis).

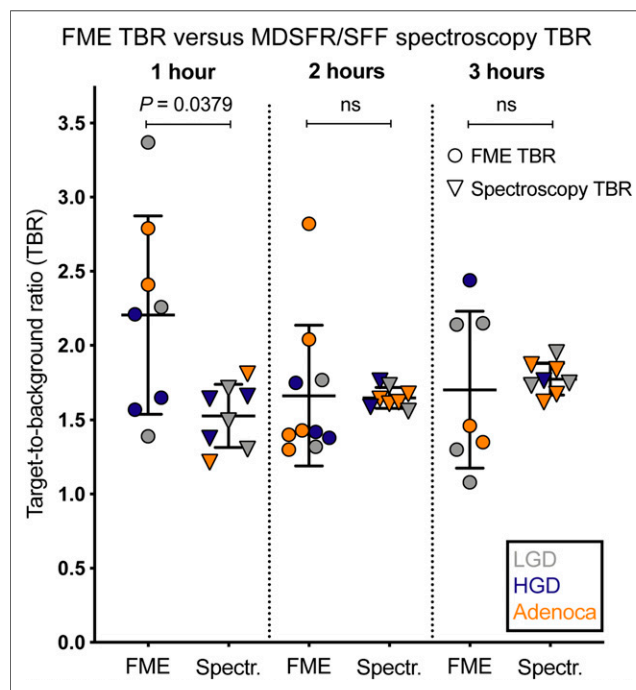


**FIGURE 4.** Median TBRs of FME images and MDSFR/SFF spectroscopy data per time cohort. Histologic grade of adenoma is low-grade dysplasia (LGD; gray), high-grade dysplasia (HGD; blue), and adenocarcinoma (Adenoca; orange). Error bars indicate median values  $\pm$  IQR (FME TBRs) and mean  $\pm$  SD (MDSFR/SFF spectroscopy TBRs).



When FME TBRs were compared with MDSFR/SFF spectroscopy TBRs, no statistically significant differences were observed, except for the 1-h cohort, in which the FME TBRs were higher than the MDSFR/SFF spectroscopy TBRs (2.18 vs. 1.54,  $P = 0.038$ ; Fig. 4). The MDSFR/SFF spectroscopy values that were corrected for the tissue scattering and absorption coefficients showed less variation than the values of the FME images.

### Ex Vivo Validation

The correlation between fluorescence intensities, histology, and c-Met expression was further evaluated ex vivo. In accordance with the in vivo results, dysplastic or cancerous mucosa showed significantly increased fluorescence compared with the surrounding normal mucosa on 4- $\mu\text{m}$  tissue sections for each cohort, with a median TBR of 1.69 (IQR, 0.49;  $P = 0.0398$ ), 1.43 (IQR, 0.37;  $P = 0.0020$ ), and 1.46 (IQR, 0.16;  $P = 0.0156$ ) for the 1-, 2-, and 3-h cohorts, respectively (Fig. 5A).

c-Met immunohistochemical analysis demonstrated a moderate (2+, 72.2%) to strong (3+, 27.8%) membrane overexpression in dysplastic mucosa, whereas normal colorectal mucosa showed a negative (0+, 53.8%) to weak (1+, 46.2%) physiologic membrane staining (Fig. 5B).

Finally, fluorescence microscopy showed increased fluorescence intensities in the dysplastic or cancerous colorectal crypts, compared with surrounding normal colorectal crypts (Fig. 5C). The fluorescence signal clearly accumulated near the cell membranes of the dysplastic cells. Surrounding normal tissue showed significantly lower fluorescence intensities, with a more stromal localization.

To further investigate EMI-137 binding specificity, in vitro experiments were performed. Immunohistochemistry and western blotting confirmed c-Met expression in HT-29 cells and minimal c-Met expression in SW-480 cells. Fluorescence microscopy

revealed EMI-137–derived fluorescence on the surface of the HT-29 cells, whereas SW-480 cells showed negligible levels of fluorescence (Supplemental Figs. 1A and 1B). Flow cytometry analysis confirmed a dose-dependent membrane binding of EMI-137 in HT-29 cells, in contrast to SW-480 cells. This finding was supported by a c-Met receptor saturation experiment using EMI-137 and the nonfluorescent unlabeled peptide (AH111972), showing blocking of the c-Met receptors and, consequently, significantly lower MFIs only in the HT-29 cells (Supplemental Fig. 1C).

### DISCUSSION

In this study, we demonstrated that FME using a 0.13 mg/kg dose of EMI-137 administered 1, 2, or 3 h before colonoscopy appears to be safe and feasible for the detection of colorectal polyps. In vivo FME results were confirmed by quantification of intrinsic fluorescence using MDSFR/SFF spectroscopy, showing significantly higher fluorescence in all lesions than in surrounding normal colorectal tissue at each time interval. No clinically significant differences were observed between the investigated time cohorts on the basis of extensive in vivo and ex vivo analyses. Therefore, we conclude that FME using EMI-137 can be performed within a 1- to 3-h time frame, thus expanding the clinical applicability of EMI-137.

The use of FME to improve polyp detection by serving as a red-flag endoscopic imaging technique has been previously investigated using different fluorescent tracers, though several factors have hampered further clinical translation (9,10). First, the near-infrared fluorescent tracer bevacizumab-800CW targeting vascular endothelial growth factor-A (peak emission, 792 nm) has unfavorable pharmacokinetics that require a dose-to-imaging interval of 2–3 d, which limits application in a colorectal cancer screening population (10). Second, the fluorescent peptide KCC\*-fluorescein

isothiocyanate (peak emission, 519 nm), which binds to sessile serrated adenomas with a V600E point-mutation in BRAF, was evaluated using postprocessing software. However, the need for postprocessing software limits real-time lesion identification in parallel to HD-WLE (9). In addition, the fact that KCC\*-fluorescein isothiocyanate has a peak emission in the visible-light spectrum may reduce imaging specificity as it has a lower penetration depth and is increasingly influenced by autofluorescence compared with near-infrared fluorescent imaging. Besides intravenous administration, topical tracer administration also has been evaluated during colonoscopy, although topical administration rarely achieves complete mucosal coverage and tracer binding is affected by bowel preparation adequacy (18). To overcome these limitations, we used a near-infrared fluorescent peptide with a relatively low molecular weight, and therefore favorable pharmacokinetic properties, that allows adenoma identification within a time frame of 1 to at least 3 h after intravenous administration.

To identify the best dose-to-imaging interval, quantification of fluorescence is important in early-phase clinical FME trials, since fluorescence intensities observed by FME

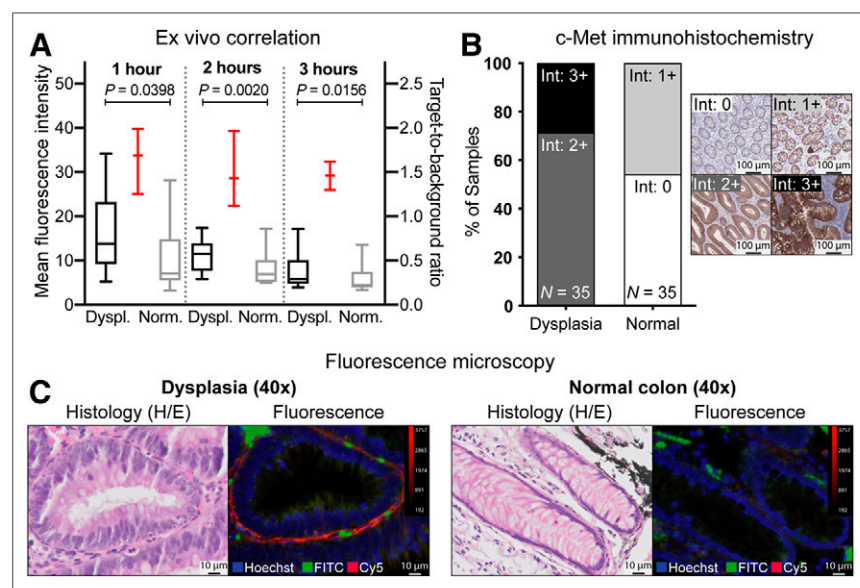


**FIGURE 5.** Ex vivo validation of EMI-137 fluorescence. (A) Correlation of mean fluorescence intensities of adenomatous (Dyspl.) and surrounding normal tissue (Norm.) with histology on 4- $\mu\text{m}$  tissue sections ( $n = 35$ ), with median values  $\pm$  IQR (left y-axis) and median TBRs (right y-axis; red). (B) c-Met membrane expression related to histology, with 0 = negative, 1+ = weak, 2+ = moderate, and 3+ = strong membrane expression. (C) Fluorescence microscopy of dysplasia (left) and normal colorectal tissue (right) ( $\times 40$  magnification; 4',6-diamidino-2-phenylindole/Hoechst nuclei staining [blue]; fluorescein isothiocyanate [FITC]/autofluorescence [green] and cyanine-5 [Cy5]/EMI-137–derived fluorescence [red]).



alone are affected by tissue optical properties and technical factors such as camera sensitivity, imaging distance, and illumination heterogeneity (19). The addition of MDSFR/SFF spectroscopy as a confirmatory technique provides objective and consistent intrinsic fluorescence values through direct-contact measurements that are corrected for the scattering and absorption coefficients of the tissue (10,13–15). The significance of using MDSFR/SFF spectroscopy was emphasized in the 3 adenomas that were qualitatively assessed to have the same fluorescence as the background during FME, whereas MDSFR/SFF spectroscopy measurements showed a significant difference in intrinsic fluorescence values. Although MDSFR/SFF spectroscopy measurements are currently calculated using a postprocessing algorithm, the results of this study further support the development of MDSFR/SFF spectroscopy measurements as a technique complementary to FME.

In line with the literature, our immunohistochemical analysis confirmed that c-Met is indeed a suitable marker for colorectal adenoma detection, as we observed a clear c-Met membrane overexpression in dysplastic and cancerous mucosa (11,12). Although there is heterogeneity in the c-Met overexpression in the adenomas, this did not influence the macroscopic fluorescence imaging results (Fig. 5). In vivo visualized and quantified fluorescence intensities remained consistent over time, indicating specific binding of EMI-137. In addition, the quantified intrinsic fluorescence values did not seem to further increase after 1 h (Fig. 2B), suggesting that the current dose of 0.13 mg/kg already saturates the available c-Met receptors 1 h after administration. Interestingly, the background fluorescence levels slightly decreased over time, as was presumably caused by clearance of unbound EMI-137 (clearance half-life, ~2h30m) (8). A lower tracer dose might further decrease background fluorescence while still saturating the available c-Met receptors, thereby potentially enhancing TBRs and improving sensitivity.

To date, integrated videoendoscopes that enable highly sensitive near-infrared fluorescence imaging in parallel to HD-WLE have not been developed. We applied a near-infrared fluorescent endoscopy system that has the potential to be used clinically, since the use of the fiber-based SurgVision Endoscope Explorer enabled simultaneous HD-WLE and FME. This use required installation of a short-pass filter in the standard Olympus white-light source; this filter prevents excitation of EMI-137 by the Olympus white-light source due to an overlap with the excitation spectrum of EMI-137. The SurgVision Endoscope Explorer fiber probe consists of 10,000 fibers, allowing sufficient resolution for colocalizing fluorescence intensities to HD-WLE images for the current study design. However, increasing the number of fibers to 30,000 would improve white-light image quality and facilitate further clinical translation of EMI-137 during screening colonoscopies (10,15,16). In addition, the red laser-light was visible on the HD-WLE images from the clinical videoendoscope, influencing HD-WLE image quality. This is a phenomenon that has not been described previously for bevacizumab-800CW, a fluorescent tracer that emits fluorescence further in the near-infrared light spectrum (10,15,16). Alternatively, installation of a short-pass filter in the tip of the endoscope or pulsed acquisition could also prevent the interference of the red-laser light during HDWLE.

In this study, FME was used to visualize fluorescence during endoscopy, whereas MDSFR/SFF spectroscopy was used to quantify intrinsic fluorescence values by correcting for tissue optical properties. Ultimately, clinicians need a technique that provides real-time objective information, preferably by combining these methods in vivo, to reliably guide the endoscopist during screening colonoscopies.

As the aim of this study was to determine the optimal dose-to-imaging interval for EMI-137, only patients with an advanced adenoma detected during a previous colonoscopy were included. As a result, a complete colonoscopy was not performed. In addition, our study population may not be representative of a screening population of patients at average risk of developing colorectal cancer. Although our cohorts were relatively small, the 3 + 3 study design is a commonly used method to acquire information on the dosing or timing of a new compound while limiting the number of exposed patients (20). A future study will need to determine whether EMI-137 can indeed improve the current adenoma detection rate in a larger general screening population.

## CONCLUSION

This study showed that FME using EMI-137 appears to be safe and feasible from a dose-to-imaging interval of 1 h to at least 3 h. Ultimately, a trade-off may be required between maintaining an adequate TBR for lesion detection and a clinically acceptable dose-to-imaging interval. Our data support further research on the potential benefit of EMI-137 within this time frame in phase II or III clinical trials, to investigate the potential improvement in polyp detection rates in a general screening population.

## DISCLOSURE

Wouter Nagengast received an unrestricted research grant from SurgVision B.V. (Groningen, the Netherlands). The study was funded by Edinburgh Molecular Imaging Ltd. (EMI), Edinburgh, United Kingdom. The funder of the study had no influence on data collection, analysis, or interpretation or in writing of the manuscript. The corresponding author had full access to all data and had final responsibility for the decision to submit for publication. No other potential conflict of interest relevant to this article was reported.

## ACKNOWLEDGMENTS

We would like to thank the patients who participated in the clinical study and Gert Jan Meersma, senior lab analyst, for performing the in vitro experiments.

## KEY POINTS

**QUESTION:** What is the optimal dose-to-imaging interval for FME using the c-Met-targeted fluorescent peptide EMI-137 for colorectal polyp detection?

**PERTINENT FINDINGS:** In this clinical trial, we showed that FME using EMI-137 appears to be safe and feasible for the detection of colorectal adenomas within a 1- to 3-h dose-to-imaging interval, based on in vivo visualization of fluorescence, in vivo quantification of fluorescence through correction for tissue optical properties, and an extensive ex vivo validation.

**IMPLICATIONS FOR PATIENT CARE:** Our findings expand the dose-to-imaging window for the clinical application of EMI-137 and support further research on EMI-137 within this time frame to improve the polyp detection rate in a general screening population.

## REFERENCES

1. Arnold M, Sierra MS, Laversanne M, Soerjomataram I, Jemal A, Bray F. Global patterns and trends in colorectal cancer incidence and mortality. *Gut*. 2017;66:683–691.
2. Leslie A, Carey F, Pratt N, Steele R. The colorectal adenoma–carcinoma sequence. *Br J Surg*. 2002;89:845–860.



3. Segnan N, Senore C, Andreoni B, et al. Baseline findings of the Italian multi-center randomized controlled trial of “once-only sigmoidoscopy”—SCORE. *J Natl Cancer Inst.* 2002;94:1763–1772.
4. Atkin W, Wooldrage K, Parkin MD, et al. Long term effects of once-only flexible sigmoidoscopy screening after 17 years of follow-up: the UK flexible sigmoidoscopy screening randomised controlled trial. *Lancet.* 2017;389:1299–1311.
5. Stoffel EM, Turgeon KD, Stockwell DH, et al. Missed adenomas during colonoscopic surveillance in individuals with Lynch syndrome (hereditary nonpolyposis colorectal cancer). *Cancer Prev Res (Phila).* 2008;1:470–475.
6. van Rijn JC, Reitsma JB, Stoker J, Bossuyt PM, van Deventer SJ, Dekker E. Polyp miss rate determined by tandem colonoscopy: a systematic review. *Am J Gastroenterol.* 2006;101:343–350.
7. Bressler B, Paszat LF, Vinden C, Li C, He J, Rabeneck L. Colonoscopic miss rates for right-sided colon cancer: a population-based analysis. *Gastroenterology.* 2004;127:452–456.
8. Burggraaf J, Kamerling IM, Gordon PB, et al. Detection of colorectal polyps in humans using an intravenously administered fluorescent peptide targeted against c-Met. *Nat Med.* 2015;21:955–961.
9. Joshi BP, Dai Z, Gao Z, et al. Detection of sessile serrated adenomas in the proximal colon using wide-field fluorescence endoscopy. *Gastroenterology.* 2017;152:1002–1013.e9.
10. Hartmans E, Tjalma J, Linssen MD, et al. Potential red-flag identification of colorectal adenomas with wide-field fluorescence molecular endoscopy. *Theranostics.* 2018;8:1458–1467.
11. Bradley CA, Dunne PD, Bingham V, et al. Transcriptional upregulation of c-MET is associated with invasion and tumor budding in colorectal cancer. *Oncotarget.* 2016;7:78932–78945.
12. Organ SL, Tsao M-S. An overview of the c-MET signaling pathway. *Ther Adv Med Oncol.* 2011;3(suppl):S7–S19.
13. van Leeuwen-van Zaane F, Gamm U, van Driel P, et al. In vivo quantification of the scattering properties of tissue using multi-diameter single fiber reflectance spectroscopy. *Biomed Opt Express.* 2013;4:696–708.
14. Hoy CL, Gamm UA, Sterenborg HJ, Robinson DJ, Amelink A. Method for rapid multidiameter single-fiber reflectance and fluorescence spectroscopy through a fiber bundle. *J Biomed Opt.* 2013;18:107005.
15. Tjalma JJ, Koller M, Linssen MD, et al. Quantitative fluorescence endoscopy: an innovative endoscopy approach to evaluate neoadjuvant treatment response in locally advanced rectal cancer. *Gut.* 2020;69:406–410.
16. Nagengast WB, Hartmans E, Garcia-Allende PB, et al. Near-infrared fluorescence molecular endoscopy detects dysplastic oesophageal lesions using topical and systemic tracer of vascular endothelial growth factor A. *Gut.* 2019;68:7–10.
17. Esfahani SA, Heidari P, Kim SA, et al. Optical imaging of mesenchymal epithelial transition factor (MET) for enhanced detection and characterization of primary and metastatic hepatic tumors. *Theranostics.* 2016;6:2028–2038.
18. Keller R, Winde G, Terpe H, Foerster E, Domschke W. Fluorescence endoscopy using a fluorescein-labeled monoclonal antibody against carcinoembryonic antigen in patients with colorectal carcinoma and adenoma. *Endoscopy.* 2002;34:801–807.
19. Koch M, Symvoulidis P, Ntziachristos V. Tackling standardization in fluorescence molecular imaging. *Nat Photonics.* 2018;12:505–515.
20. Le Tourneau C, Lee JJ, Siu LL. Dose escalation methods in phase I cancer clinical trials. *J Natl Cancer Inst.* 2009;101:708–720.